論 文

[2208] Micromechanical Model for Triaxial Behavior of Concrete

Ahmed M. FARAHAT *1, Masashi KAWAKAMI *2 and Tada-aki TANABE *3

1. INTRODUCTION

The early phenomenological macroscopic models for concrete are based on an almost never-ending process of modifications of the classical theories. However, it is very difficult to imagine that many aspects of the material response can be easily modeled by a unified general theory in which the real mechanical response of the material microstructure is not involved. Thus, the utility of the phenomenological macroscopic models for concrete is at best of limited value. Alternatively, an approach, which is known as the microscopic approach and is based on the local view of the material properties, seems to be more promising. This paper focuses on the microscopic approach.

In the present study, a micromechanical model which can precisely predict the triaxial behavior of concrete is formulated. The current model is an extension of the model which was originally introduced by Farahat, Wu and Tanabe [3, 4] to predict the monotonic and cyclic behavior of concrete in the two-dimensional domain. The microcracking, which is the most relevant cause of non-linearity, is assumed to be localized at the thin as well as the thick mortar layers between coarse aggregates. For this purpose, concrete is idealized to have two kinds of contacts, aggregate-aggregate and aggregate-mortar contacts. The behavior of these contacts is defined and distinguished. Finally, an explicit formula which expresses the tangent stiffness matrix of the material as a summation of the contributions of all contacts at the different thicknesses, inside the representative volume, is derived. The basic assumptions of the proposed model were experimentally verified [9]. The proposed model is in contrast to Bazant's microplane model [1] in which the microcracks are assumed to be localized only in the thin layers of mortar and no experimental work has been conducted to verify the fundamental assumptions of the model. Finally, comparative results between the available test data and the analytical results are included. The proposed model has shown its capability to verify accurately all test data.

[1]* Nagoya University (Dept. of Civil and Environmental Engineering, Kumamoto University)
[2]* Konoike Construction Company
[3]* Department of Civil Engineering, Nagoya University

2. THEORETICAL CONSIDERATION

2.1 AVERAGE STRESS TENSOR FROM AVERAGES CONTACT FORCES

In order to consider the microcracks at the thin and the thick layers of mortar, concrete is idealized to have two types of particles; aggregate and mortar particles. Moreover, every mortar particle is assumed to be surrounded by aggregate particles. This idealization enables us to observe the behavior not only at aggregate-aggregate contacts, i.e. thin layers of mortar, which has been studied by Bazant et al. [1] but also at aggregate-mortar contacts, i.e. thick layers of mortar. Using the average volume of stresses [8], if $\Delta\sigma_{ij}$ is the stress state which is in equilibrium, the average stresses $\Delta\bar{\sigma}^a_{ij}$ and $\Delta\bar{\sigma}^m_{ij}$ within an aggregate and mortar particles can be written as follows [3, 4, 8]:

$$\Delta\bar{\sigma}^a_{ij} = \frac{1}{v^a}\int_{v^a}\Delta\sigma_{ij}dv \quad \text{.....} \quad (1\text{–}a) \qquad \Delta\bar{\sigma}^m_{ij} = \frac{1}{v^m}\int_{v^m}\Delta\sigma_{ij}dv \quad \text{.....} \quad (1\text{–}b)$$

where v^a and v^m are the volumes of an aggregate and mortar particles, respectively. The macroscopic mean stress $\Delta\bar{\sigma}_{ij}$ for any representative volume can be obtained by summing the stresses within the internal particles as follows [3, 4, 9]:

$$\Delta\bar{\sigma}_{ij} = \frac{1}{V}\left[\sum_a \Delta\bar{\sigma}^a_{ij}\, v^a + \sum_m \Delta\bar{\sigma}^m_{ij}\, v^m\right] \tag{2}$$

in which V is the total volume, $\sum_a$ and $\sum_m$ represent the summation of all aggregate and mortar particles, respectively. Using the divergence theory and the equilibrium condition (i.e. $\Delta\sigma_{ij,j} = 0$), the volume integral in eq.(1) can be converted to surface integral which can be replaced by the summation of the discrete boundary tractions. If the results obtained are substituted in eq.(2), the macroscopic mean stresses in eq.(2) can be simplified as follows [3, 4]:

$$\Delta\bar{\sigma}_{ij} = \frac{1}{V}\Big(\sum_{C_1}\Delta f_i^{C_1} l_j^{C_1} + \sum_{C_2}\Delta f_i^{C_2} l_j^{C_1} + \sum_{C_2}\Delta f_i^{C_2} l_j^{C_2}\Big) \tag{3}$$

where C_1 and C_2 are the total number of contacts between aggregates alone and between aggregate and mortar particles. f_i and l_j are the contact force and the contact vector at any contact. If the contacts are grouped within a finite number of orientational intervals, the grouped average $\Delta\bar{f}\bar{l}(\Omega)$ in eq.(3) can be calculated. To consider the distribution of the orientation of contacts, the function $E(\Omega)$ is defined. This function considers the relative frequency of contacts with different orientations of normals. The number of contacts with normals between Ω and $\Omega + \Delta\Omega$ is $CE(\Omega)\Delta\Omega$ (C is the total number of contacts). Since the current study considers concrete as an isotropic material, this function was defined [8] to be equal to $E(\Omega) = 1/4\pi$. For a large number of contacts and very small orientational intervals, eq.(3) can be written in the next integral form [3, 4]:

$$\Delta\bar{\sigma}_{ij} = \frac{C_1\bar{l}_1}{V}\int_\Omega \Delta\bar{f}_i^{C_1}(\Omega)\, n_j^{C_1}(\Omega)E(\Omega)d\Omega + \frac{C_2\bar{l}_1}{V}\int_\Omega \Delta\bar{f}_i^{C_2}(\Omega)\, n_j^{C_1}(\Omega)E(\Omega)d\Omega + \frac{C_2\bar{l}_2}{V}\int_\Omega \Delta\bar{f}_i^{C_2}(\Omega)\, n_j^{C_2}(\Omega)E(\Omega)d\Omega \tag{4}$$

where $\bar{l}_1$ and $\bar{l}_2$ are the average radii of the aggregate and mortar particles, respectively.

2.2 AVERAGE CONTACT FORCES - STRAIN TENSOR RELATIONSHIP

In the beginning the contact force vector $\Delta \bar{f}_i^c$ is decomposed into normal and shear force components as follows:

$$\Delta \bar{f}_i^c(\Omega) = \Delta(\bar{f}_n^c(\Omega))_i + \Delta(\bar{f}_t^c(\Omega))_i \tag{5}$$

Using the contact law, the normal and shear force vectors are linked with the corresponding normal and shear strain vectors at the contact as shown in Fig.1 as follows:

$$\Delta(\bar{f}_n^c(\Omega))_i = K_N \, \Delta \, (\varepsilon_n)_i \tag{6}$$

$$\Delta(\bar{f}_t^c(\Omega))_i = K_S \, \Delta \, (\varepsilon_t)_i \tag{7}$$

It has been found experimentally [9] that the local normal strains for a group of contacts with the same orientation can be considered as the resolved components of the macroscopic strain tensor. Therefore, the following relations can be easily obtained:

$$\Delta(\varepsilon_n)_i = n_i \, n_k \, n_l \, \Delta \bar{\varepsilon}_{kl} \tag{8}$$

$$\Delta(\varepsilon_t)_i = [\, \delta_{ik} \, n_l - n_i \, n_k \, n_l \,] \, \Delta \bar{\varepsilon}_{kl} \tag{9}$$

Substituting eqs.(8) and (9) into eqs.(6) and (7) and the resulting value into eq.(5), the following results can be obtained:

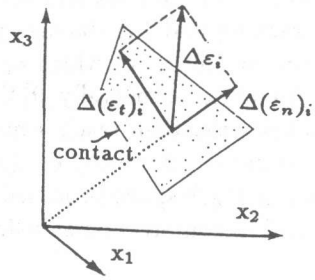

(a) Strain Components

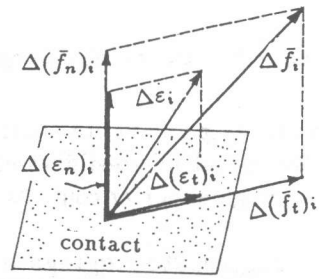

(b) Force Components

Fig.1 Strain and Force Components at the Contact

$$\Delta \bar{f}_i^c(\Omega) = [\, K_N \, n_i \, n_k \, n_l + K_S \, \{\, \delta_{ik} \, n_l - n_i \, n_k \, n_l \,\} \,] \, \Delta \bar{\varepsilon}_{kl} \tag{10}$$

in which K_N and K_S are the normal and shear stiffnesses at the contact, n are the direction cosines of the unit normal to the contact. δ_{ik} is the Kronecker's unit delta tensor.

2.3 INCREMENTAL MACROSCOPIC STRESS- STRAIN RELATIONSHIP

By substituting eq.(10) into eq.(4), the following incremental macroscopic stress-strain relationship can be obtained:

$$\Delta \bar{\sigma}_{ij} = D_{ijkl} \, \Delta \bar{\varepsilon}_{kl} \tag{11}$$

where $D_{ijkl} = \eta_1 \int_\Omega [\, k_n^{c_1} \, n_i \, n_j \, n_k \, n_l + k_s^{c_1} \, \{\, \delta_{ik} \, n_j \, n_l - n_i \, n_j \, n_k \, n_l \,\} \,] \, d\,\Omega +$

$$\eta_2 \int_\Omega [\, k_n^{c_2} \, n_i \, n_j \, n_k \, n_l + k_s^{c_2} \, \{\, \delta_{ik} \, n_j \, n_l - n_i \, n_j \, n_k \, n_l \,\} \,] \, d\,\Omega \tag{12}$$

with $\eta_1 = C_1 \, \bar{l}_1 \bar{a}_1 / 4 \, \pi \, V, \qquad \eta_2 = C_2 \, \bar{l}_1 \bar{a}_2 / 4 \, \pi \, V + C_2 \, \bar{l}_2 \bar{a}_2 / 4 \, \pi \, V,$

$$k_n^{c_1} = K_N^{c_1} / \bar{a}_1, \quad k_n^{c_2} = K_N^{c_2} / \bar{a}_2, \quad k_s^{c_1} = K_S^{c_1} / \bar{a}_1, \quad k_s^{c_2} = K_S^{c_2} / \bar{a}_2$$

Both $(c_1, \bar{a}_1)$ and $(c_2, \bar{a}_2)$ refer to the contacts and the average contact areas between aggregate-aggregate and aggregate-mortar particles. k_n and k_s are the normal and shear stiffnesses which can be obtained from the normal microscopic stress-strain relationship. In this study k_s is assumed to be linear with k_n (i.e. $k_s = \lambda k_n$).

2.4 NORMAL STRESS-STRAIN RELATION OF THE CONTACTS

Aggregate - Mortar Contact: The stress strain relation for the contact relating σ_n to ε_n, must describe the cracking and the damage all the way to complete fracture or failure, at which σ_n reduces to zero. It has been found experimentally [9] that σ_n as a function of ε_n must first rise, then reach a maximum, and then gradually decline. However, eqs.(13) and (14), which are shown in Fig.2-a, are proposed for the contacts in tension and in compression as follow:

$$for\ \varepsilon_n \geq 0 \quad \sigma_n = E_2\ \varepsilon_n\ exp[\ -(\frac{E_2}{E_1})^p\ (\frac{\varepsilon_n}{\varepsilon_t})^p] \qquad (13)$$

$$for\ \varepsilon_n > 0 \quad \sigma_n = E_2\ \varepsilon_n\ exp[\ -|\frac{\varepsilon_n}{\varepsilon_c}|^{p_1}] \qquad (14)$$

where ε_t, ε_c ,p and p_1 are material constants, E_1 and E_2 are the initial micro-stiffnesses of aggregate-aggregate and aggregate-mortar contacts, respectively.

Aggregate-Aggregate Contact: The normal stress-strain relationships proposed by Bazant et al.[1] are used here. These relations are given in eqs.(15) and (16) and shown in Fig.2-b.

$$for\ \varepsilon_n \geq 0 \quad \sigma_n = E_1\ \varepsilon_n\ exp[\ -(\frac{\varepsilon_n}{\varepsilon_t})^p] \qquad (15)$$

$$for\ \varepsilon_n < 0 \quad \sigma_n = -C_1 + C_2 tan^{-1}[C_3(\varepsilon_n\ -\ C_4)] \qquad (16)$$

where, $C_1 = -0.27 f_c'$, $C_2 = 0.87 f_c'$, $C_3 = 1.15(\frac{E_1}{f_c'})$, and $C_4 = -\frac{1}{C_3}\ tan\ (\frac{C_1}{C_2})$

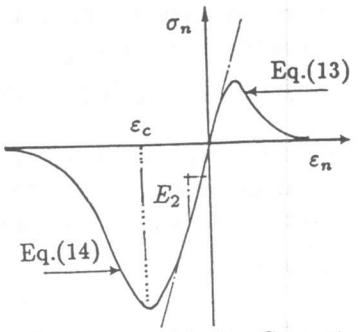

(a) Aggregate-Mortar Contact

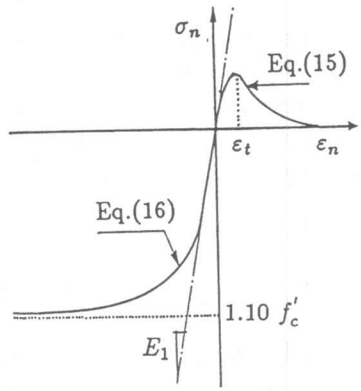

(b) Aggregate-Aggregate Contact

Fig.2 Stress-Strain Relationship at the Contacts

3. THE RELATION BETWEEN MACRO AND MICRO VARIABLES

If the macroscopic strain tensor $\bar{\varepsilon}_{ij}$ is assumed to correspond to uniaxial strains, i.e. $\bar{\varepsilon}_z \neq 0$ and $\bar{\varepsilon}_x = \bar{\varepsilon}_y = 0$, and by using the spherical coordinates, the corresponding macroscopic stresses can be calculated. Comparing the results with Hooke's law, the following relations can be found:

$$\nu = \frac{1\ -\ \lambda}{4\ -\ \lambda} \text{ .....(17-a)} \qquad E = \frac{4\pi}{15}(3+2\lambda)(\eta_1 E_1 + \eta_2 E_2) \text{.....(17-b)}$$

in which ν and E are the macroscopic elastic Poisson's ratio and Young's modulus. λ, E_1, E_2, η_1, and η_2 are microscopic characteristic variables which were defined before. In the numerical calculation, the proposed algorithm by Bazant et al.[1] is used. Based on this algorithm [1], the integral of eq.(12) can be obtained as follows:

$$\int_\Omega F\ d\ \Omega = 2\ \left[\ 4\ \pi\ \sum_{\alpha}^{N}\ w_\alpha\ F_\alpha\ \right] \qquad (18)$$

in which subscript α refers to set of directions in space and w_α are the weights(numerical integration coefficients). In all analysis, eq.(18) with N=21 directions is used.

4. VERIFICATION OF THE PROPOSED MODEL

In the beginning, reasonable values of the parameters, which describe the characteristic properties of the contacts, are selected as follows, $p = p_1$=2.5(eqs.(13), (14) and (15)), ν=0.18(eq.(17-b)), η_1/η_2=0.10, $\eta_1 + \eta_2 = 1$ and E_1/E_2=1.80 [3, 4]. These values were kept constant in all calculations. Finally, only ε_t and ε_c in eqs.((13), (14) and (15)) are considered to be variable parameters. A sample of the results is shown in Figs.3, 4 and 5. Fig.3 shows the comparison between the uniaxial (tension and compression) test data and the model results. In Fig.3-a (uniaxial tension), the value of $\varepsilon_c = 0.0016$ (eq.(14)) is kept constant and the value of ε_t (eqs.(13) and (15)) was estimated by eq.(19-a) [3, 4]. In eq.(19-a), f_t and E are the macroscopic tensile strength and Young's Modulus. In Fig.3-b (uniaxial compression), the value of ε_t=1.5x10^{-3} (eqs.(13), (15)) is kept constant and the value of ε_c was estimated by eq.(19-b) [3, 4]. In eq.(19-b), f_c' and E are the macroscopic compressive strength and Young's Modulus of concrete.

$$\varepsilon_t = (f_t/E)^{1.006} \quad \text{.....(19-}a\text{)}$$

$$\varepsilon_c = (f_c'/E)^{0.944} \quad \text{.....(19-}b\text{)}$$

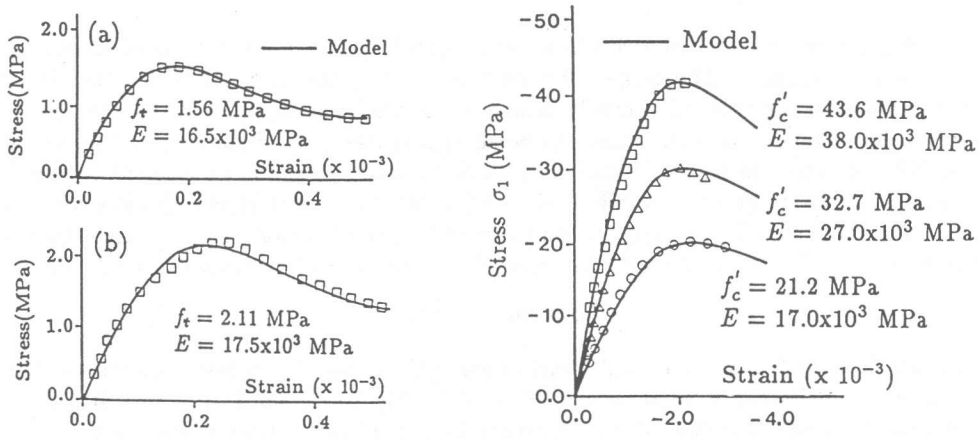

(a) Uniaxial Tension [2] (b) Uniaxial Compression [5]

Fig.3 Comparison with Uniaxial Test Data

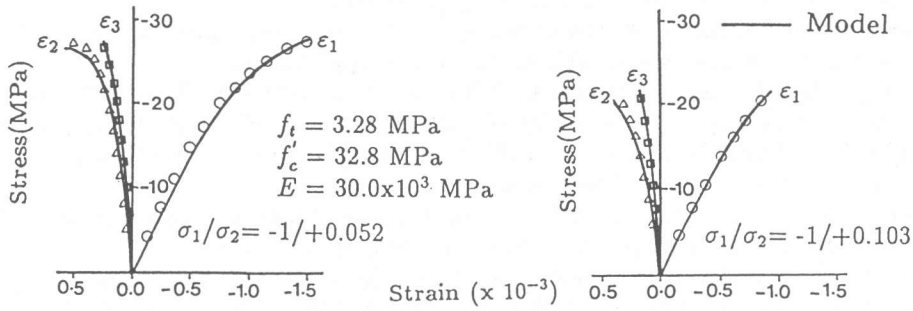

Fig.4 Comparison with Biaxial Tension-Compression Test Data of Ref.[7]

Figs.4 and 5 show the comparison with the biaxial and triaxial test data. In Figs.4 and 5, the values of ε_c and ε_t were calculated using eq.(19). The two variables satisfy the uniaxial behavior (tension and compression) of concrete.

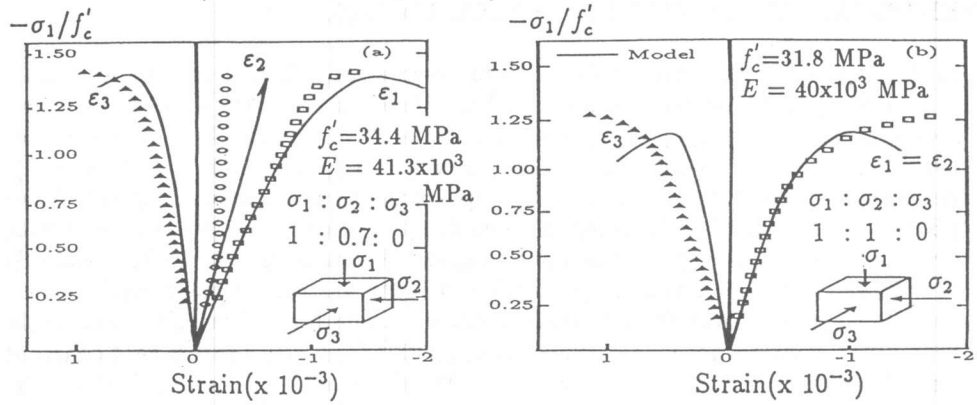

Fig.5 Comparison with the Test Data of Ref.[6]

5. CONCLUSIONS

A micromechanical model which can accurately predict the triaxial behavior of concrete is developed. The proposed model is constructed in order to accurately consider all possible sorts of microcracks which are apparently localized at the thin as well as the thick layers of mortar between coarse aggregates. The behavior at the contacts with different thicknesses is defined and distinguished. Finally, an explicit formula of the stiffness matrix as the contribution of all contacts with different thicknesses is derived. The conceptual simplicity of the proposed model is rewarded by ease of material identification. The model showed its capability to predict the available test data.

REFERENCES

1. Bazant, Z. P. and Gambarova, P.," Crack Shear in Concrete : Crack Band Microplane Model for," *Journal of Structural Engineering, ASCE*, Vol. 111, No. 4, April 1985, pp. 2015-2035.

2. Evans, R. H. and Marathe, M. S. ,"Microcracking and Stress-Strain Curves of Concrete in Tension," *Material and Structure (Paris)*, No. 1, 1968, pp. 61-64.

3. Farahat, A.M., Wu, Z.S. and Tanabe, T.,"Development of Microplane Model of Concrete with Plural Types of Granular Particles," *Proc. of JSCE*, 1991, No.433/V-15, pp. 231-238.

4. Farahat, A. M., Wu, Z. S. and Tanabe, T. ,"Modified Cyclic Micromechanical Model for Concrete," *Proc. of JSCE*, 1992, No.451/V-17, pp. 301-311.

5. Hognestad, E., Hanson, N. W. and Mchenry, D. ,"Concrete Stress Distribution in Ultimate Strength Design," *Journal of ACI*, Vol. 52, No. 4, 1955, pp. 455-477.

6. Linhua, J., Dahai, H. and Nianxiang, X. , "Behavior of Concrete under Triaxial Compressive-Compressive-Tensile Stresses," *Journal of ACI Material*, Vol. 88, No. 2, 1991, pp. 181-185.

7. Kupfer, H., Hilsdorf, H. K. and Rusch, H. ,"Behavior of Concrete under Biaxial Stresses," *Journal of ACI*, Vol. 66, No. 8, 1969, pp. 656-666.

8. Routhenburg, L. and Bathurst, R. J.,"Analytical Study of Induced Anisotropy in Idealized Granular Material," *Geotechnique*, Vol. 39, No. 4, 1989, pp. 601-614.

9. Yamada, K., Kawakami, M., Farahat, A. M. and Niwa, J. ,"An Experimental Study on Micromechanical Failure of Concrete," *Proceeding of JCI*, 1993 (Submitted for Publication).